Original paper

Folia Neuropathologica

Inhibition of poly (ADP-ribose) polymerase 1 in neuron cells might enhance the therapeutic effect of leonurine under cholesterol stimulation

Bo Hou[1*], Zhigang Huan[2*], Chao Zhang[3*], Zhiyong Chen[4], Lingmei Ha[5], Shengxuan Huang[4]

[1]Neurosurgery Department, Zibo First Hospital, Zibo, Shandong, China, [2]Neurology Department, Zibo First Hospital, Zibo, Shandong, China, [3]Neurosurgery Department, Tianjin Union Medical Center, China, [4]Neurosurgery Department, Sanming First Hospital Affiliated to Fujian Medical University, Sanming, Fujian, China, [5]Emergency Department, Characteristic Medical Center of PAP, Tianjin, China

*Bo Hou, Zhigang Huan and Chao Zhang contribute equally in this work.

Folia Neuropathol 2022; 60 (1): 76-91 *DOI: https://doi.org/10.5114/fn.2022.114355*

Abstract

Atherosclerosis (AS) is a chronic inflammatory disease with high morbidity and mortality worldwide and is the pathologic basis of cerebral-cardiovascular disease. Cerebral infarction is caused by cerebral ischemia in the deep brain stem or cerebral hemisphere, and small vessel atherosclerosis is the pathophysiological basis of lacunar cerebral infarction. In this study, we found that inhibition of PARP1 in neuronal cells increased the proliferation rate of cells, reduced the concentration of cholesterol in neuronal cells, inhibited the expression and secretion of proinflammatory factors and promoted the expression and secretion of proangiogenic factors. In addition, the reverse transport process of cholesterol and autophagy process were activated in neuron cells by detecting the target proteins using western blotting analysis, and further experiments found that this process might be mediated by activation of the PI3K/AKT/mTOR signalling pathway. Thus, we thought inhibition of PARP1 might be a new therapeutic method for cerebral-cardiovascular disease.

Key words: *leonurine, cholesterol, neuron cell, PARP1, PI3K/AKT/mTOR.*

Introduction

Atherosclerosis is an inflammatory disease that occurs in the arterial wall and is characterized by progressive accumulation of lipids and inflammatory cells in the intima of large arteries [2]. Internalization of lipids in the intima is the first stage of atherosclerosis, which, combined with endothelial activation or dysfunction [26], further secretes chemotactic and growth factors, induces the migration, accumulation and proliferation of VSMCs and leukocytes, promotes the formation of atherosclerotic plaques, and the accumulation of cholesterol is a critical risk factor for cerebral artery atherosclerosis, which has been considered a consistent association between cholesterol concentration and ischemic stroke [19]. Leonurine is an effective constituent extracted from Herba Leonuri, which is widely distributed in Africa, Asia, Europe and North America and presents an

Communicating authors

Shengxuan Huang, Neurosurgery Department, Affiliated Sanming First Hospital of Fujian Medical University, No. 29 Liedong St., Sanming, Fujian, China, 365000, e-mail: huangshengxuan2008@163.com; Lingmei Ha, Emergency Department, Characteristic Medical Center of PAP, No. 220 Chenglin Road, Tianjin, China, 300162, e-mail: 1527632513@qq.com

anti-inflammatory, antinociceptive and hypoglycaemic function. A previous study found that activation of poly (ADP-ribose) polymerase 1 (PARP1) reduces the level of NAD+, resulting in a reduction in cellular ATP levels and leading to cell death [3]. Inhibition of PARP1 using pharmacological methods has been found in the treatment of experimental models of atherosclerosis [32]. Proatherogenic conditions, including oxidized low-density lipoprotein (oxLDL), immunogenic lipopolysaccharides (LPS), hyperglycaemia, angiotensin II (Ang-II), H_2O_2 and peroxynitrite [34,48], induce the production of free radicals and oxidants in vascular cells *via* activation of PARP1, leading to the development of atherosclerosis. In this study, we established a PARP1 overexpression and inhibition cell model in HT-22 and GT1-7 cells and found that inhibition of PARP1 in HT-22 and GT1-7 cells decreased the cellular concentration of cholesterol and inhibited the inflammatory process and the concentration of proangiogenic cytokines. We further noticed that inhibition of PARP1 increased the expression of AGCA1, ABCG1, Beclin1 and Atg5 with a decrease in the expression of Toll-like receptors, activated the cholesterol reverse transport process and autophagy process and inhibited the inflammatory response process. In addition, we further found that these effects might be mediated by activation of the PI3K/AKT/mTOR signalling pathway. Thus, we thought that inhibition of PARP1 might be a therapeutic method for cerebral vessel disease.

Material and methods

Material

Leonurine (SML0670) was purchased from Sigma. PJ34 (HY-13688A) was purchased from MCE. Cholesterol was purchased from Sigma (C4951). Lipofectamine 3000 Transfection Reagent (L3000150), TRIzol Plus RNA Purification Kit (12183555), Maxima First Strand cDNA Synthesis Kit (K1671) and PowerUp SYBR Green Master Mix (A25742) were purchased from Thermo. The Total Cholesterol Content Assay Kit (BC1980) and MTT (M8180) were purchased from Solarbio. DMEM (670087) and fetal bovine serum (FBS) (10099) were purchased from Gibco. Anti-phosphoinositide-3-kinase (PI3K, ab74136), protein kinase B (AKT, ab179463), p-AKT (ab38449), mechanistic target of rapamycin kinase (mTOR, ab2732), p-mTOR (ab109268), nuclear factor-κB p65 (NF-κB p65, ab16502), p-NF-κB (ab86299), IKK (ab178870), Toll-like receptors 2 (TLR2, ab209217), TLR4 (ab22048), ATP binding cassette subfamily A member 1 (ABCA1, ab18180), ATP binding cassette subfamily G member 1 (ABCG1, ab52617), vascular endothelial growth factor α (VEGF-α, ab52917), fibroblast growth factor 2 (FGF2, ab92337), Beclin1 (ab207612) and autophagy-related 5 (ATG5, ab108327) were purchased from Abcam. VEGF-α (ab100751), FGF (ab100670), interleukin (IL)-1β (ab100704), and IL-10 (ab108870) ELISA kits were purchased from Abcam. HEK293T (CRL-1573) cells were purchased from American Type Culture Collection (ATCC).

Ethical review

Not applicable for there are no animal or human trials.

Vector construction

To construct the PARP1 overexpression vector, the PAPR1 fragment was amplified using PCR with the following primers: forward: 5'- AACCTCTAGAATGGCGGAGTCTTCGGATAAG-3', reverse: 5'- AACCGCGGCTTAAGCGTAGTCTGGGACGTCGTATGGGTACCACAGGGAGGTCTTAAAATTG-3', and cloned into the pCDH-CMV-Puro vector. Plasmid transfection was performed according to the protocol of Lipofectamine 3000 Transfection Reagent. HT-22 and GT1-7 cells were infected with lentiviral supernatants for 48 h, and stable cell lines were selected using 2 μg/ml puromycin.

Cell culture and grouping

HT-22 (SCC129) and GT1-7 (SCC116) cells were purchased from the Cell Bank of the Chinese Academy of Sciences and cultured at 37°C in a humidified atmosphere supplied with 5% CO_2 and cultured in DMEM with 10% FBS. Cells were divided into four groups: the normal group (NC), leonurine treatment group (CH), leonurine treatment supplied with PARP1 inhibition group (CA) and leonurine treatment supplied with PARP1 overexpression group (CI). In all groups, cells were first treated with 100 μg/ml cholesterol for 12 h [51]. In the leonurine treatment groups, cells were first treated with 80 μM leonurine for 24 h, and in the PARP1 inhibition group, cells were treated with 1 μM PJ34 for 24 h [50]. After treatment, cells were collected for further experiments.

MTT assay

Cells were seeded into a 96-well plate at a concentration of 10^5 and treated as previously described. After treatment, cells were incubated with MTT reagent at a concentration of 5 mg/ml for 4 h, and then cultured medium was removed (n = 3). The optical density at 490 nm was detected using a Multiskan FC microplate reader after incubation with DMSO for 10 min.

RNA extraction and reverse transcription

RNA extraction was performed according to the protocol of the TRIzol Plus RNA Purification Kit. Cells were first lysed and homogenized with TRIzol reagent followed by incubation at room temperature for 5 min. After mixing with chloroform and incubation for 5 min, samples were centrifuged at 12,000 g for 15 min, and the RNA in aqueous phase was removed into a new tube. Then, samples were mixed with an equant volume of ethanol and bound to the membrane in a collection tube using centrifugation. After washing with washing buffer, the RNA was eluted with elution buffer, and the concentration of RNA was determined using a Qubit 4 Fluorometer (Thermo). The reaction mixture of reverse transcription was made up as recommended and incubated at 25°C for 10 min, 50°C for 15 min and 85°C for 5 min. Then, cDNA samples were stored at –80°C until performing the following experiments.

Quantitative polymerase chain reaction (qPCR)

The reaction mixture was made up as recommended. The experiment was performed using the following steps: UDG activation for 2 min at 50°C and dual-lock DNA polymerase for 2 min at 95°C. These steps were repeated for 40 cycles: denaturation for 15 s at 95°C, annealing for 15 s at 58°C and extension for 1 min at 72°C. In addition, the primers used were listed as follows: IL-1β, Forward: 5'-GCTGCTTCCAAACCTTTGAC-3', Reverse: 5'-AGCTTCTCCACAGCCACAAT-3'; IL-6, Forward: 5'-CCTCTGGCGGAGCTATTGAG-3', Reverse: 5'-CGGCAAGTGAGCAGATAGCA-3'; IL-10, Forward: 5'-GGAGGTGCTGCTTGTGACAG-3', Reverse: 5'-TTGACTGCTGGCGATATGCT-3'; NLRP3, Forward: 5'-GGAGGTGCTGCTTGTGACAG-3', Reverse: 5'-TGCCACCTTCTGACCAGTGT-3'; TLR4, Forward: 5'-GCATGGCTTACACCACCTCTC-3', Reverse: 5'-TGTCTCCACAGCCACCAGAT-3'; TLR2, Forward: 5'-GCAGTCCCAAAGTCTAAAGTCG-3', Reverse: 5'-CTACGGGCAGTGGTGAAAAC-3'. The expression of mRNA was measured using the 2-ΔΔCq method [24]. GAPDH was used as an internal control (n = 3).

Protein extraction and western blotting analysis

Cells were lysed with RIPA buffer supplemented with proteinase inhibitor cocktail, and the concentration of proteins was determined using a BCA assay. Then, 60 µg protein samples were used to perform the western blotting analysis. Samples were loaded and separated using 10% SDS-PAGE electrophoresis, and then protein samples were transferred onto nitrocellulose membranes using the Trans-Blot Turbo Transfer System. Membranes were first incubated with 5% skim milk for 1 h at room temperature and incubated with primary antibodies at 4°C overnight. The grey values of each band were detected using a chemiluminescent immunoassay after incubation with secondary antibody for 1 h at room temperature. The grey value of each target protein in each group was analysed using Image-Pro Plus software (version 6.0). GAPDH was used as an internal control. The expression level of each target protein was calculated by the grey value and then normalized to the grey value of the corresponding GAPDH grey value of each group.

Measurement of total cholesterol levels in HT-22 and GT1-7 cells

Total cholesterol levels in HT-22 and GT1-7 cells were detected using a total cholesterol content assay kit. Cells were first counted using a cell counter, and the same number of cells (10^6) was used to perform the following experiment. According to the protocol, cells were lysed using lysis buffer followed by ultrasound for 3 min. After centrifugation at 10,000 g for 10 min at 4°C, samples and standards were added to each well of a 96-well plate and incubated with working solution, and the concentration of cellular total cholesterol was detected at 500 nm using a Multiskan FC microplate reader.

Enzyme-linked immunosorbent assay

The enzyme-linked immunosorbent assay (ELISA) experiment was performed according to the protocol. Briefly, cultured medium and standard samples

were loaded into each well and incubated for 2 h at room temperature with ante shaking. After washing with washing buffer, samples were incubated with substrate solution and stop solution, and the optical density at 405 nm was detected using a Multiskan FC microplate reader.

Statistical analysis

Data were presented as the mean ± SD. *P* values were calculated using ANOVA (n = 3, each experiment was repeated three times independently). $P < 0.05$ was set as a statistic difference. $^{*}P < 0.05$ compared with the NC group, $^{\#}p < 0.05$ compared with the CH group.

Results

Effect of PARP1 inhibition on the proliferation of HT-22 and GT1-7 cells

As shown in Figure 1A, the viability rates of HT-22 cells in the CH, CI and CA groups were 73.3 ±7.1, 58.2 ±5.8 and 95.6 ±9.3, respectively. The viability rates of GT1-7 cells in the CH, CI and CA groups were 68.5 ±6.7, 52.1 ±4.8 and 87.6 ±8.3, respectively. The viability rate in the CH and CI groups was significantly decreased compared with that in the NC group ($p < 0.05$), significantly increased in the CA group and significantly decreased in the CI group ($p < 0.05$) compared with that in the CH group in both HT-22 and GT1-7 cells. We also detected the expression of PARP1 in these groups without treatment with cholesterol (Fig. 1B). The expression of PARP1 in the NC, CA and CI groups of HT-22 cells was 1.26 ±0.10, 0.59 ±0.05, and 1.89 ±0.15, respectively. The expression of PARP1 in the NC, CA and CI groups of GT1-7 cells was 0.08 ±0.01, 0.04 ±0.01 and 0.12 ±0.01, respectively. The expression of PARP1 in the CA group was significantly decreased and significantly increased in the CI group compared with the NC group ($p < 0.05$), indicating that the PARP1 overexpression and inhibition group was successfully established. In Figure 1C, the concentrations of total cholesterol in HT-22 cells in the NC, CH, CI and CA groups were 0.71 ±0.05, 0.93 ±0.07, 1.20 ±0.10 and 0.76 ±0.05 μmol/l, respectively. The concentrations of cholesterol in the NC, CH, CI and CA groups were 0.53 ±0.03, 0.85 ±0.06, 1.08 ±0.08 and 0.62 ±0.04, respectively, in GT1-7. The concentration of cellular cholesterol was significantly increased in the CH and CI groups compared with the NC group ($p < 0.05$) and was significantly increased in the CI group and significantly decreased in the CA group ($p < 0.05$) compared with the CH group.

Effect of PARP1 inhibition on the secretion of inflammatory-related factors

In each group of HT-22 cells, the concentrations of VEGF-α in the culture medium of the NC, CH, CA and CI groups were 285.0 ±10.2, 321.4 ±15.4, 378.2 ±17.2 and 241.2 ±8.5 pg/ml, respectively. The concentrations of FGF in these groups were 184.2 ±9.6, 256.3 ±11.2, 292.1 ±10.8 and 145.5 ±8.1 pg/ml. The concentrations of IL-1β in these groups were 296.3 ±14.1, 274.2 ±12.4, 247.1 ±11.3 and 354.1 ±17.5 pg/ml. The concentrations of IL-10 in these groups were 0.75 ±0.06, 0.92 ±0.09, 1.23 ±0.11 and 0.42 ±0.05 ng/ml (Fig. 2). In each group of GT1-7 cells, the concentrations of VEGF-α in the culture medium of the NC, CH, CA and CI groups were 183.2 ±9.3, 235.1 ±12.5, 284.6 ±14.2 and 157.1 ±7.6 pg/ml, respectively. The concentrations of FGF in these groups were 148.6 ±6.4, 197.3 ±8.2, 277.8 ±12.4 and 124.5 ±5.1 pg/ml. The concentrations of IL-1β in these groups were 265.4 ±11.5, 231.4 ±9.8, 187.6 ±7.3 and 284.6 ±13.2 pg/ml. The concentrations of IL-10 in these groups were 0.62 ±0.03, 0.84 ±0.06, 1.17 ±0.08 and 0.36 ±0.01 ng/ml (Fig. 3). As shown in Figures 2 and 3, the concentrations of VEGF-α, FGF and IL-10 in the culture medium of HT-22 and GT1-7 cells were significantly increased in the CH and CA groups and significantly decreased in the CI group compared with the NC group ($p < 0.05$), significantly decreased in the CI group and significantly increased in the CA group compared with the CH group ($p < 0.05$). The concentration of IL-1β was significantly decreased in the CH and CA groups and significantly increased in the CI group compared with the NC group ($p < 0.05$), and compared with the CH group, the concentration of IL-1β was significantly decreased in the CA group and significantly increased in the CI group ($p < 0.05$).

Effect of PARP1 inhibition on the expression of inflammation-related genes

As shown in Figure 4, the expression of IL-1β in the NC, CH, CA and CI groups of HT-22 cells was 0.96 ±0.08, 0.81 ±0.07, 0.58 ±0.05 and 1.32 ±0.12, respectively. The expression of IL-1β was significantly

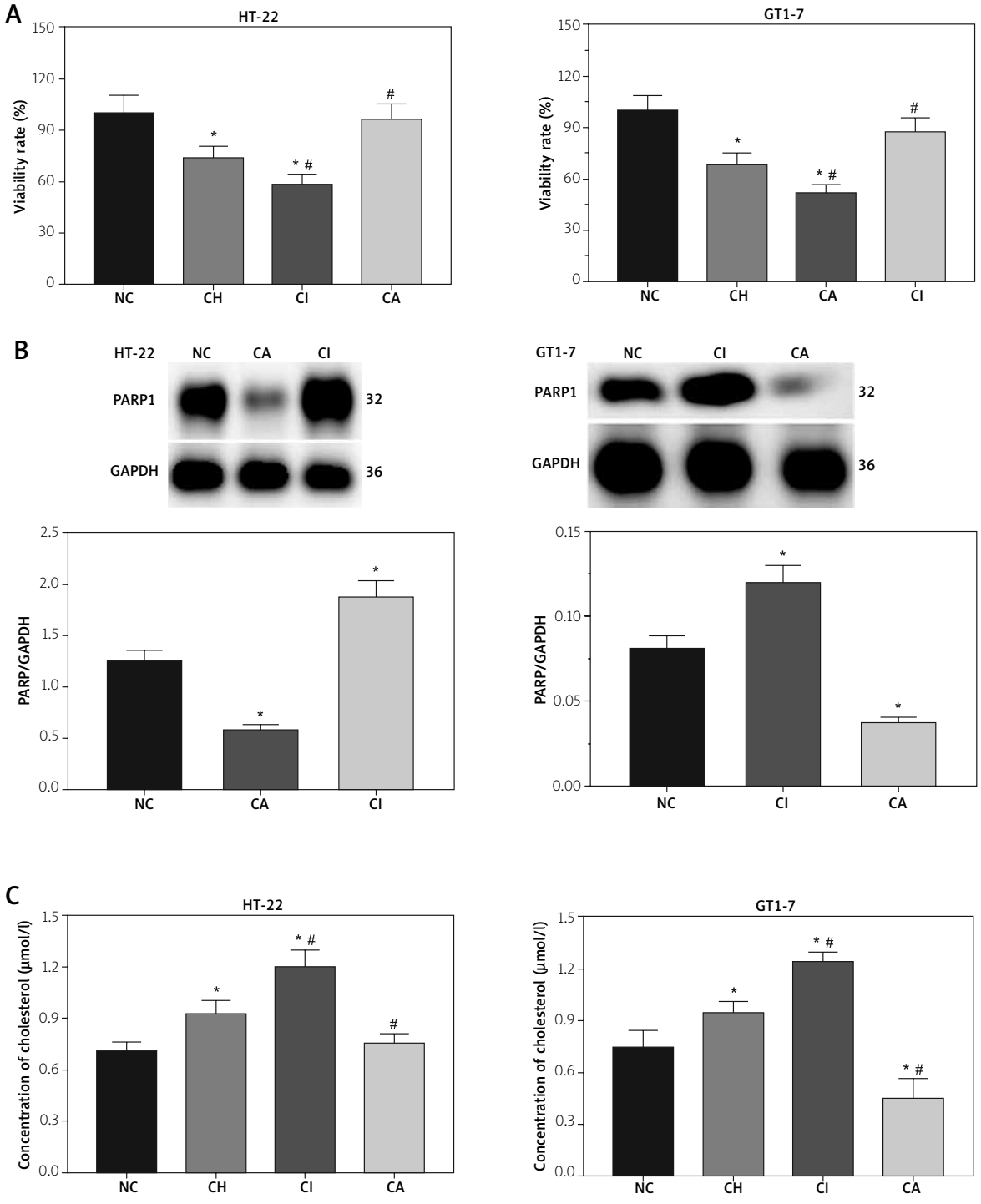

Fig. 1. The viability rate, expression of PARP1 and cellular cholesterol concentration in HT-22 and GT1-7 cells. **A**) Viability rate of HT-22 and GT1-7 cells in each group. **B**) Expression of PARP1 in each group of HT-22 and GT1-7 cells. **C**) Cellular concentration of cholesterol in each group of HT-22 and GT1-7 cells. Data were presented as the mean ± SD. Each experiment was repeated three times independently (n = 3). *p < 0.05 compared with the NC group, #p < 0.05 compared with the CH group.

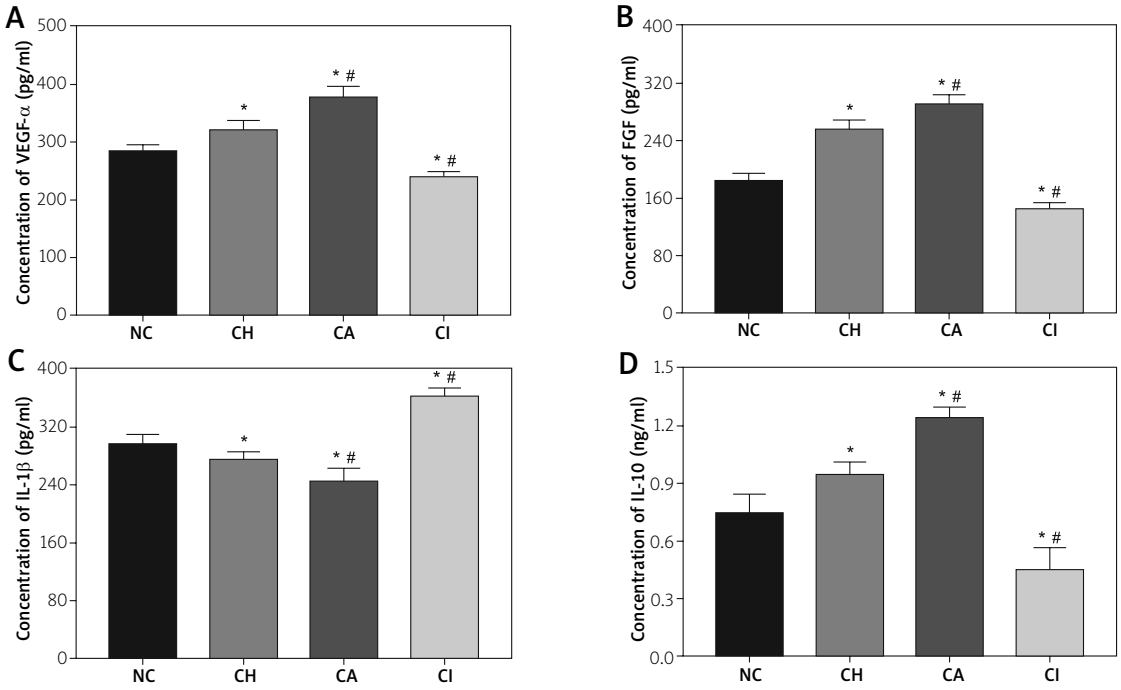

Fig. 2. Detection of the concentration of inflammatory-related factors and angiogenesis-related factors in the medium of HT-22 cells using ELISA. **A**) Concentration of VEGF-α in each group. **B**) Concentration of FGF in each group. **C**) Concentration of IL-1β in each group. **D**) Concentration of IL-10 in each group. Data were presented as the mean ± SD. Each experiment was repeated three times independently (n = 3). *p < 0.05 compared with the NC group, #p < 0.05 compared with the CH group.

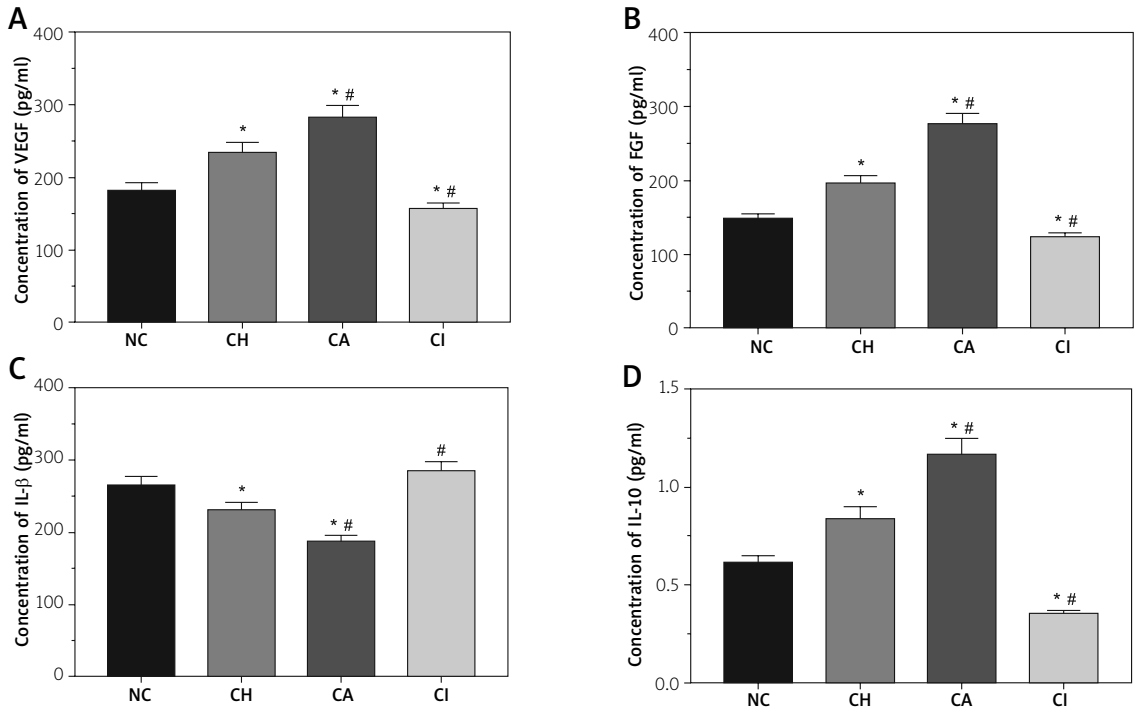

Fig. 3. Detection of the concentration of inflammatory-related factors and angiogenesis-related factors in the medium of GT1-7 cells using ELISA. **A**) Concentration of VEGF-α in each group. **B**) Concentration of FGF in each group. **C**) Concentration of IL-1β in each group. **D**) Concentration of IL-10 in each group. Data were presented as the mean ± SD. Each experiment was repeated three times independently (n = 3). *p < 0.05 compared with the NC group, #p < 0.05 compared with the CH group.

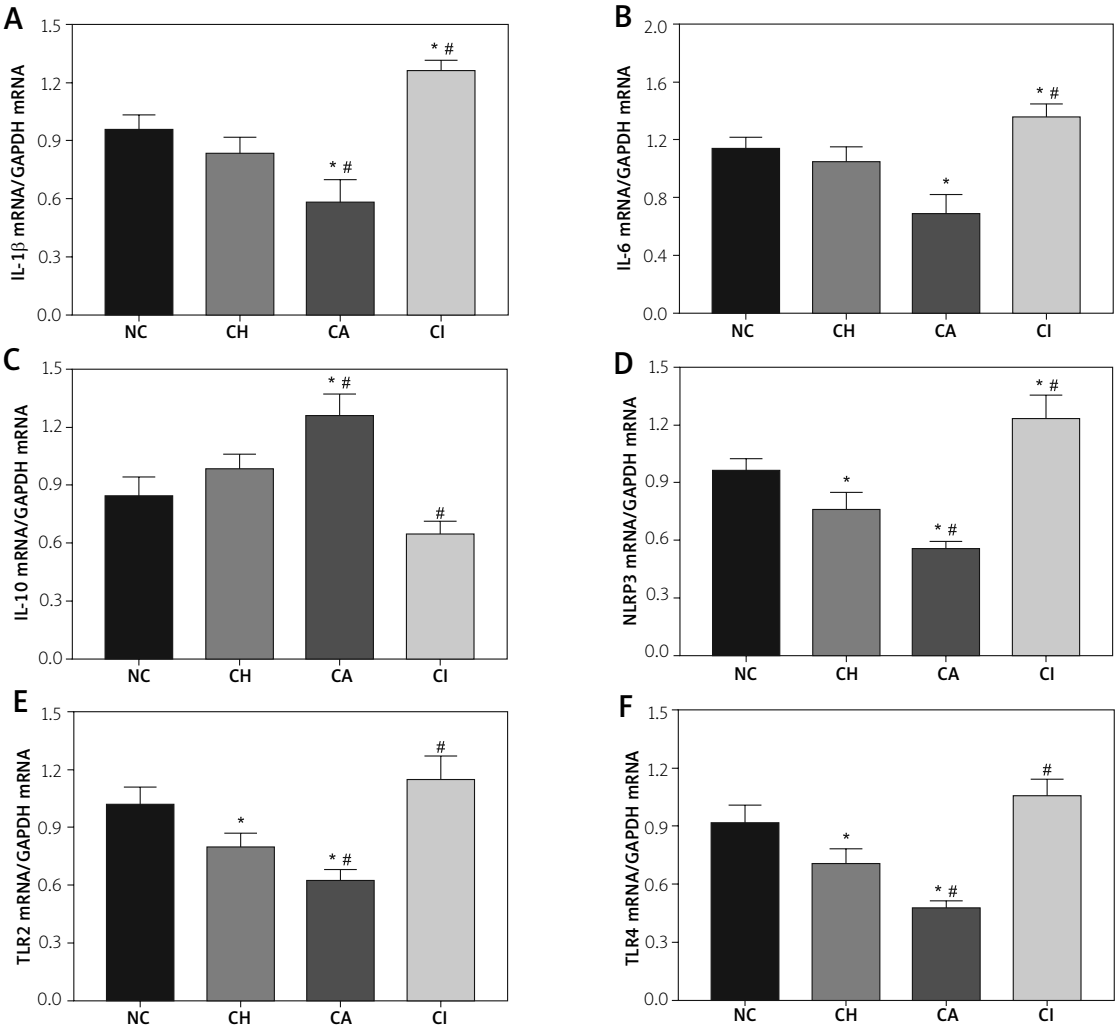

Fig. 4. Detection of the expression level of inflammation-related genes in HT-22 cells using RT-qPCR. **A**) Expression of IL-1β in each group. **B**) Expression of IL-6 in each group. **C**) Expression of IL-10 in each group. **D**) Expression of NLRP3 in each group. **E**) Expression of TLR2 in each group. **F**) Expression of TLR4 in each group. Data were presented as the mean ± SD. Each experiment was repeated three times independently (n = 3). *p < 0.05 compared with the NC group. #p < 0.05 compared with the CH group.

decreased in the CA group compared with the NC and CH groups (p < 0.05). This value was significantly increased in the CI group compared with the NC and CH groups (p < 0.05). The expression of IL-6 in these groups was 1.13 ±0.10, 0.94 ±0.08, 0.71 ±0.06 and 1.42 ±0.13. The change in IL-6 in these groups presented a trend similar to that of IL-1β. The expression of IL-10 in these groups was 0.84 ±0.07, 1.02 ±0.10, 1.34 ±0.13 and 0.61 ±0.04. The expression of IL-10 was significantly increased in the CA group compared with the NC and CH groups (p < 0.05) and was significantly decreased in the CI group compared with the CH group (p < 0.05). The expression of NLRP3 in these groups was 0.96 ±0.09, 0.73 ±0.06, 0.54 ±0.04 and 1.33 ±0.13. The expression of NLRP3 was significantly decreased in the CH and CA groups compared with the NC group (p < 0.05) and significantly increased in the CI group compared with the NC group (p < 0.05). Compared with the CH group, the expression of NLRP3 was significantly decreased in the CA group and significantly increased in the CI group (p < 0.05). The expression of TLR2 in these groups was 1.02 ±0.09, 0.80 ±0.07, 0.63 ±0.05 and 1.15 ±0.12. The expression of TLR4 in these groups

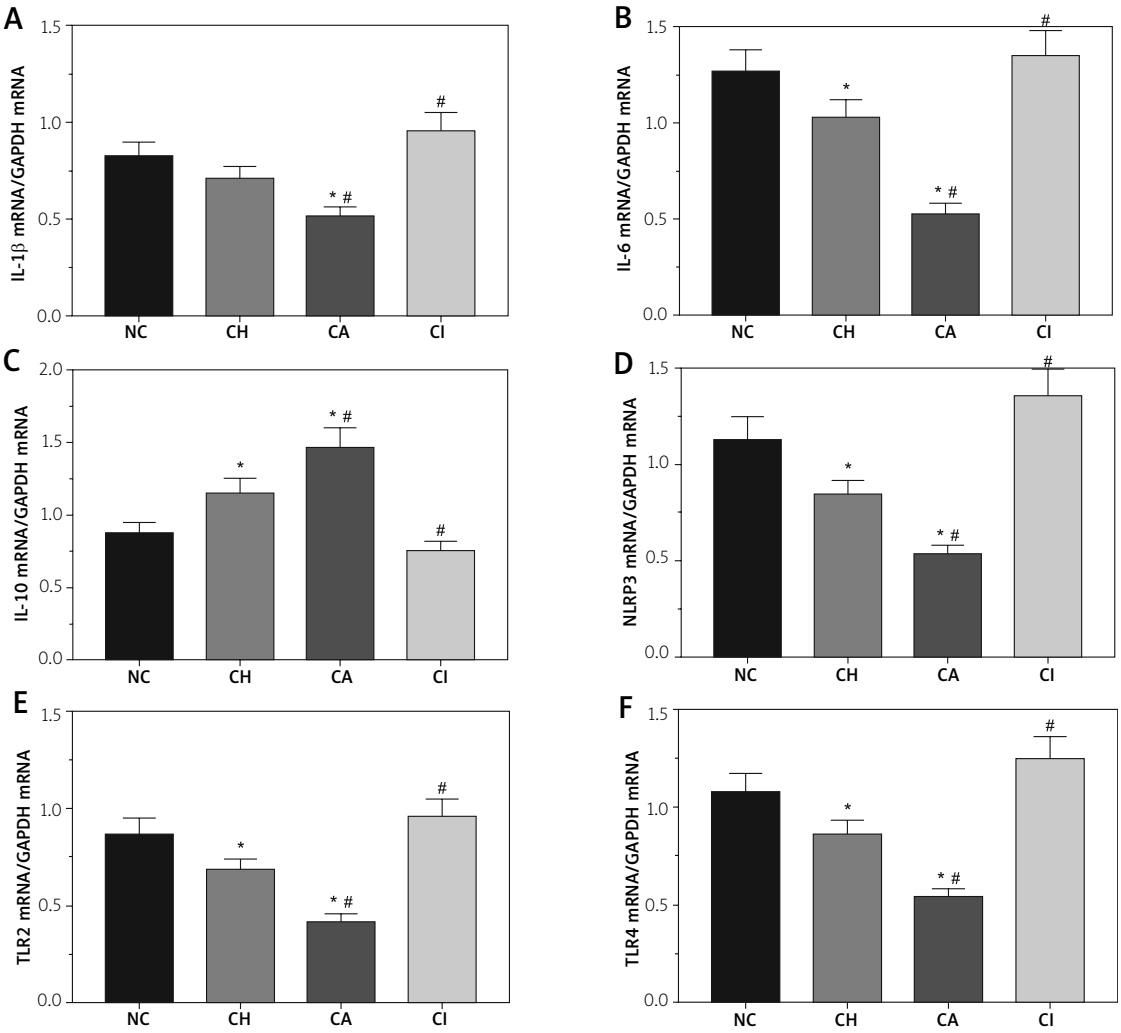

Fig. 5. Detection of the expression level of inflammation-related genes in GT1-7 cells using RT-qPCR. **A**) Expression of IL-1β in each group. **B**) Expression of IL-6 in each group. **C**) Expression of IL-10 in each group. **D**) Expression of NLRP3 in each group. **E**) Expression of TLR2 in each group. **F**) Expression of TLR4 in each group. Data were presented as the mean ± SD. Each experiment was repeated three times independently (n = 3). *p < 0.05 compared with the NC group. #p < 0.05 compared with the CH group.

was 0.92 ±0.09, 0.71 ±0.07, 0.48 ±0.03 and 1.06 ±0.08. Compared with the NC group, the expression of TLR2 and TLR4 was significantly decreased in the CH and CA groups (p < 0.05), and the expression of TLR2 and TLR4 was significantly decreased in the CA group and significantly increased in the CI group compared with the CH group (p < 0.05). In Figure 5, the expression of IL-1β in the NC, CH, CA and CI groups of GT1-7 cells was 0.83 ±0.07, 0.71 ±0.06, 0.52 ±0.04 and 0.96 ±0.09, respectively. The expression of IL-1β was significantly decreased in the CA group compared with the NC and CH groups (p < 0.05). This value was significantly increased in the CI group compared with the CH group (p < 0.05). The expression of IL-6 in these groups was 1.27 ±0.11, 1.03 ±0.09, 0.53 ±0.05 and 1.35 ±0.13. The change in IL-6 expression was significantly decreased in the CH and CA groups compared with the NC group (p < 0.05) and was significantly decreased in the CA group but significantly increased in the CI group compared with the CH group (p < 0.05). The expression of IL-10 in these groups was 0.88 ±0.07, 1.15 ±0.10, 1.47 ±0.13 and 0.76 ±0.06. The expression of IL-10 was significantly increased in the CA group compared with the NC and CH groups (p < 0.05) and was significantly decreased in the CI group compared with the

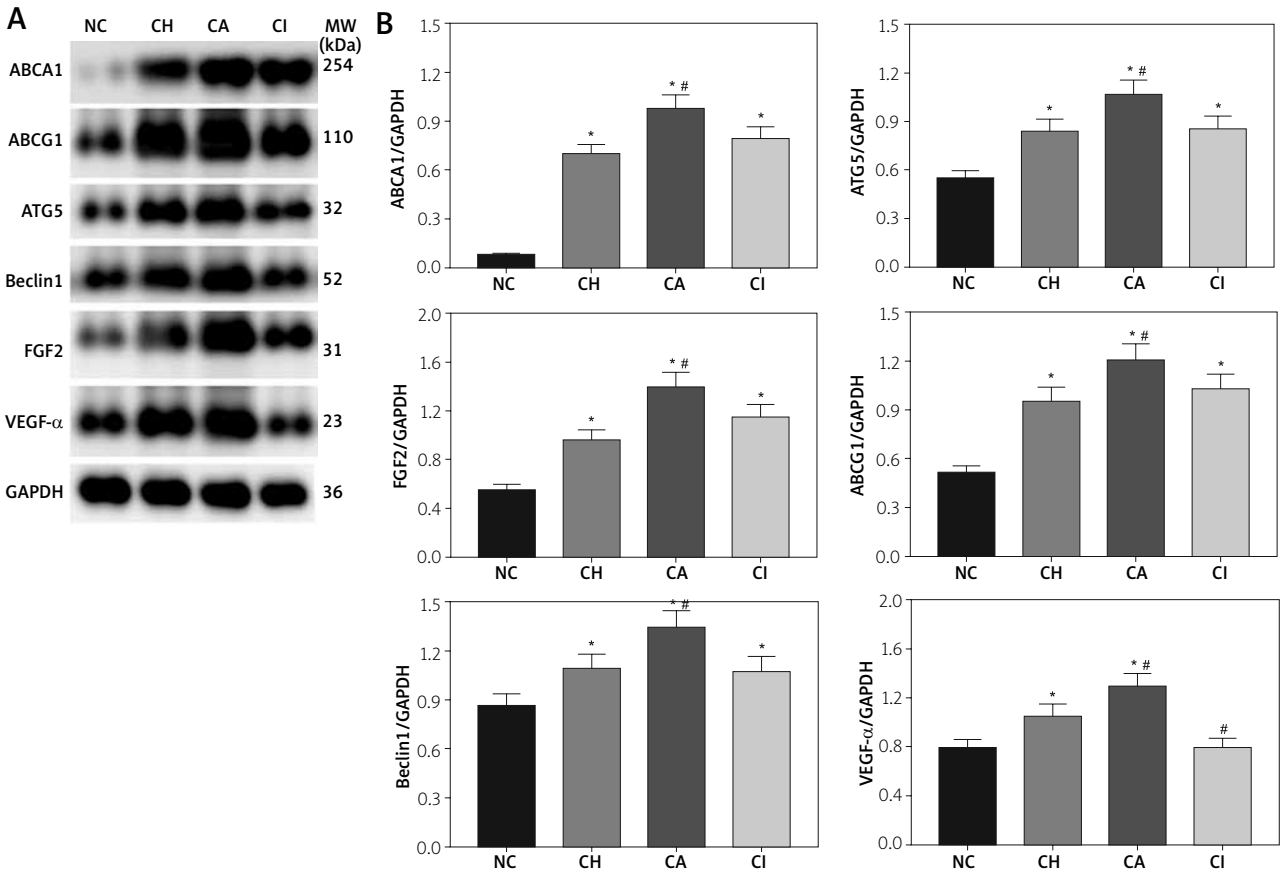

Fig. 6. Detection of the expression levels of inflammatory-, autophagy- and angiogenesis-related proteins in HT-22 cells using western blot analysis. **A**) Expression of each target proteins. **B**) Quantitative analysis of each protein. Data were presented as the mean ± SD. Each experiment was repeated three times independently (n = 3). *p < 0.05 compared with the NC group, #p < 0.05 compared with the CH group.

CH group (p < 0.05). The expression of NLRP3 in these groups was 1.13 ±0.12, 0.85 ±0.07, 0.54 ±0.04 and 1.36 ±0.14. The expression of NLRP3 was significantly decreased in the CH and CA groups compared with the NC group (p < 0.05), and compared with the CH group, the expression of NLRP3 was significantly decreased in the CA group and significantly increased in the CI group (p < 0.05). The expression of TLR2 in these groups was 0.87 ±0.08, 0.69 ±0.05, 0.42 ±0.04 and 0.96 ±0.09. The expression of TLR4 in these groups was 1.08 ±0.09, 0.86 ±0.07, 0.54 ±0.04 and 1.25 ±0.11. Compared with the NC group, the expression of TLR2 and TLR4 was significantly decreased in the CH and CA groups (p < 0.05), and the expression of TLR2 and TLR4 was significantly decreased in the CA group and significantly increased in the CI group compared with the CH group (p < 0.05).

Effect of PARP1 inhibition on the expression of cholesterol transport-related and inflammation-related proteins

As shown in Figure 6, the expression of cholesterol transport-related and inflammation-related proteins in HT-22 cells was detected using western blotting analysis. The expression of ABCA1 in the NC, CH, CA and CI groups was 0.08 ±0.01, 0.70 ±0.06, 0.98 ±0.08 and 0.79 ±0.07, respectively. Increased expression levels of ABCA1 were observed in the CH, CA and CI groups compared with the NC group (p < 0.05), and the expression of ABCA1 in the CA group was significantly increased compared with the CH group (p < 0.05). The expression of ABCG1 in these groups was 0.52 ±0.04, 1.05 ±0.09, 1.21 ±0.10 and 1.13 ±0.09. The

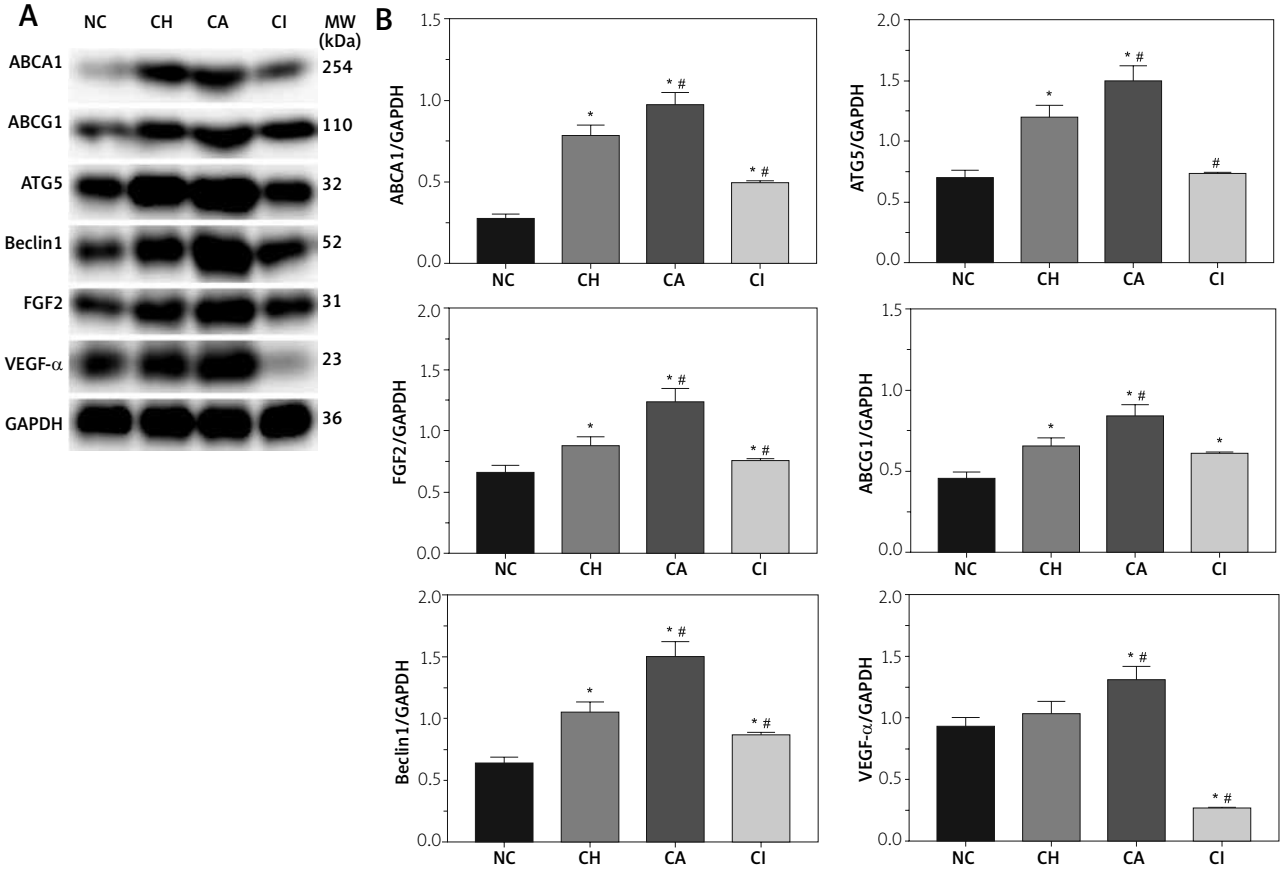

Fig. 7. Detection of the expression levels of inflammatory-, autophagy- and angiogenesis-related proteins in GT1-7 cells using western blot analysis. **A**) Expression of each target proteins. **B**) Quantitative analysis of each protein. Data were presented as the mean ± SD. Each experiment was repeated three times independently (n = 3). *p < 0.05 compared with the NC group. #p < 0.05 compared with the CH group.

expression of ATG5 in these groups was 0.55 ±0.05, 0.94 ±0.08, 1.07 ±0.09 and 0.95 ±0.08. The expression of Beclin1 in these groups was 0.86 ±0.07, 1.09 ±0.09, 1.24 ±0.10 and 1.08 ±0.09. The expression of FGF2 in these groups was 0.55 ±0.05, 0.96 ±0.08, 1.40 ±0.12 and 1.15 ±0.10. Changes in the expression of ABCG1, ATG5, Beclin1 and FGF2 presented a trend similar to that of ABCA1. The expression of VEGF-α in these groups was 0.79 ±0.07, 1.15 ±0.10, 1.20 ±0.10 and 0.80 ±0.07. Increased expression of VEGF-α was observed in the CH and CA groups compared with the NC group (p < 0.05), and increased expression of VEGF-α and decreased expression of VEGF-α were observed in the CA and CI groups compared with the CH group (p < 0.05). In Figure 7, the expression of ABCA1 in GT1-7 cells of the NC, CH, CA and CI groups was 0.28 ±0.02, 0.79 ±0.06, 0.92 ±0.07 and 0.50 ±0.004, respectively. The expression of ABCA1 was significantly increased in all treatment groups compared with the NC group (p < 0.05), was significantly increased in the CA group (p < 0.05) and was significantly decreased in the CI group compared with the CH group. The expression of ABCG1 in these groups was 0.46 ±0.04, 0.66 ±0.05, 0.85 ±0.07 and 0.62 ±0.005. The expression of ABCG1 was significantly increased in all treatment groups compared with the NC group (p < 0.05) and was significantly increased in the CA group compared with the CH group (p < 0.05). The expression of ATG5 in these groups was 0.70 ±0.05, 1.20 ±0.09, 1.51 ±0.12 and 0.74 ±0.007. The expression of ATG5 was significantly increased in the CH and CA groups compared with the NC group (p < 0.05) and was significantly increased in the CA group and decreased in the CI group (p < 0.05). The expression of Beclin1 in these groups was 0.64 ±0.05, 1.06 ±0.08, 1.51 ±0.12 and 0.87 ±0.008. The expression of Beclin1 was signifi-

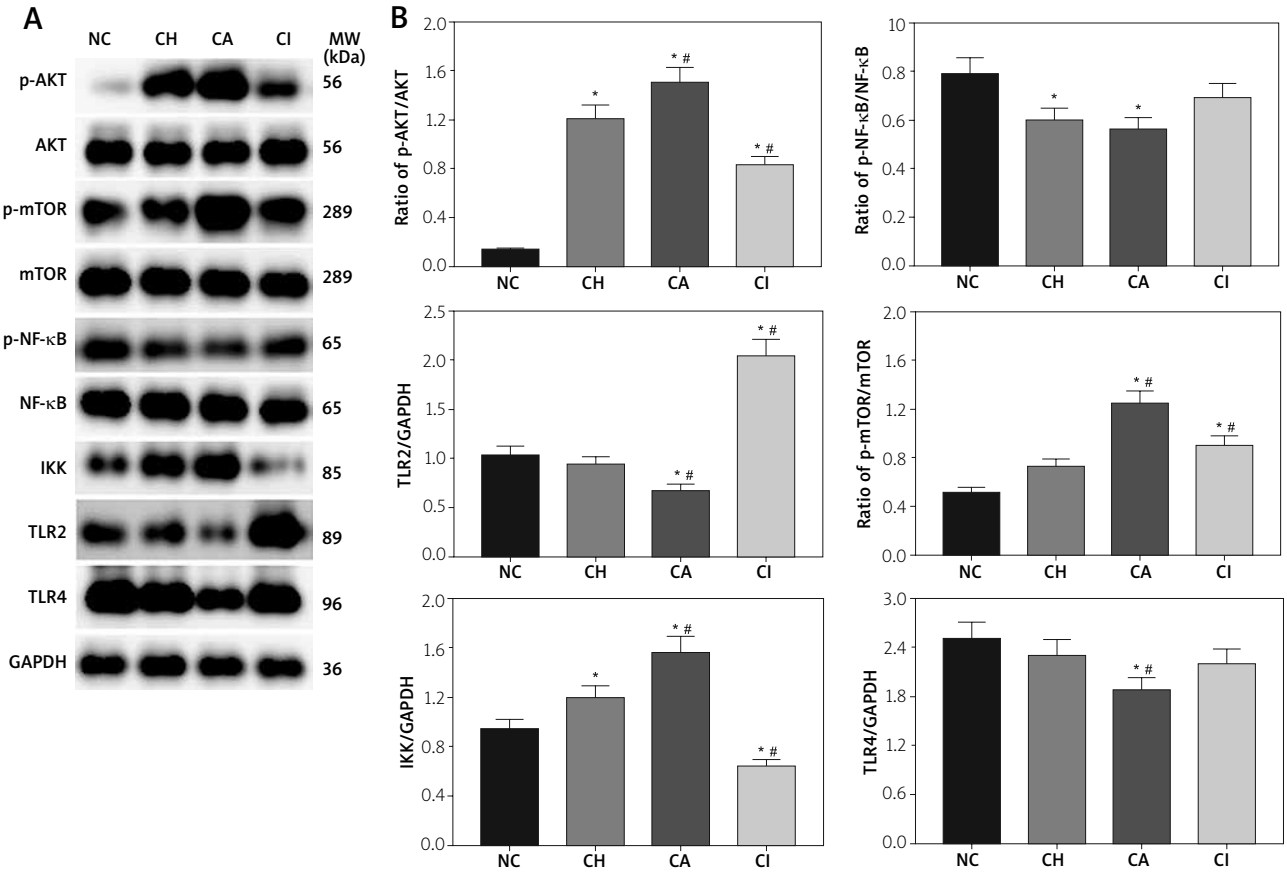

Fig. 8. Detection of activation of the PI3K/AKT/mTOR signalling pathway in HT-22 cells using western blot analysis. **A**) Expression of key molecules in the PI3K/AKT/mTOR signalling pathway. **B**) Quantitative analysis of each protein. Data were presented as the mean ± SD. Each experiment was repeated three times independently (n = 3). *p < 0.05 compared with the NC group, #p < 0.05 compared with the CH group.

cantly increased in all treatment groups compared with the NC group (p < 0.05) and was significantly increased in the CA group and decreased in the CI group compared with the CH group (p < 0.05). The expression of FGF2 in these groups was 0.67 ±0.05, 0.88 ±0.07, 1.25 ±0.10 and 0.76 ±0.006. The change in the expression of FGF2 presented a trend similar to that of Beclin1. The expression of VEGF-α in these groups was 0.94 ±0.07, 1.14 ±0.09, 1.32 ±0.10 and 0.28 ±0.002. The expression of VEGF-α was significantly increased in the CA group and significantly decreased in the CI group compared with the NC and CH groups (p < 0.05).

Effect of PARP1 inhibition on activation of the PI3K/AKT signalling pathway

As shown in Figure 8, activation of the PI3K/AKT signalling pathway was detected using western blotting analysis. The ratios of p-AKT/AKT in the NC, CH, CA and CI groups of HT-22 cells were 0.14 ±0.01, 1.21 ±0.10, 1.50 ±0.13 and 0.83 ±0.07, respectively. The PI3K/AKT ratio was significantly increased in all treatment groups compared with the NC group (p < 0.05). Compared with the CH group, the ratio of PI3K/AKT was significantly increased in the CA group and significantly decreased in the CI group (p < 0.05). The ratios of p-mTOR/mTOR in these groups were 0.51 ±0.04, 0.73 ±0.06, 1.25 ±0.10 and 0.90 ±0.08. The ratio of p-mTOR/mTOR was significantly increased in all treatment groups compared with the NC group (p < 0.05) and was significantly increased in the CA and CI groups compared with the CH group (p < 0.05). The ratios of p-NF-κB/NF-κB in these groups were 0.79 ±0.07, 0.60 ±0.05, 0.57 ±0.05 and 0.69 ±0.06. The ratio of p-NF-κB/NF-κB was significantly decreased in the CH and CA groups compared with the NC group

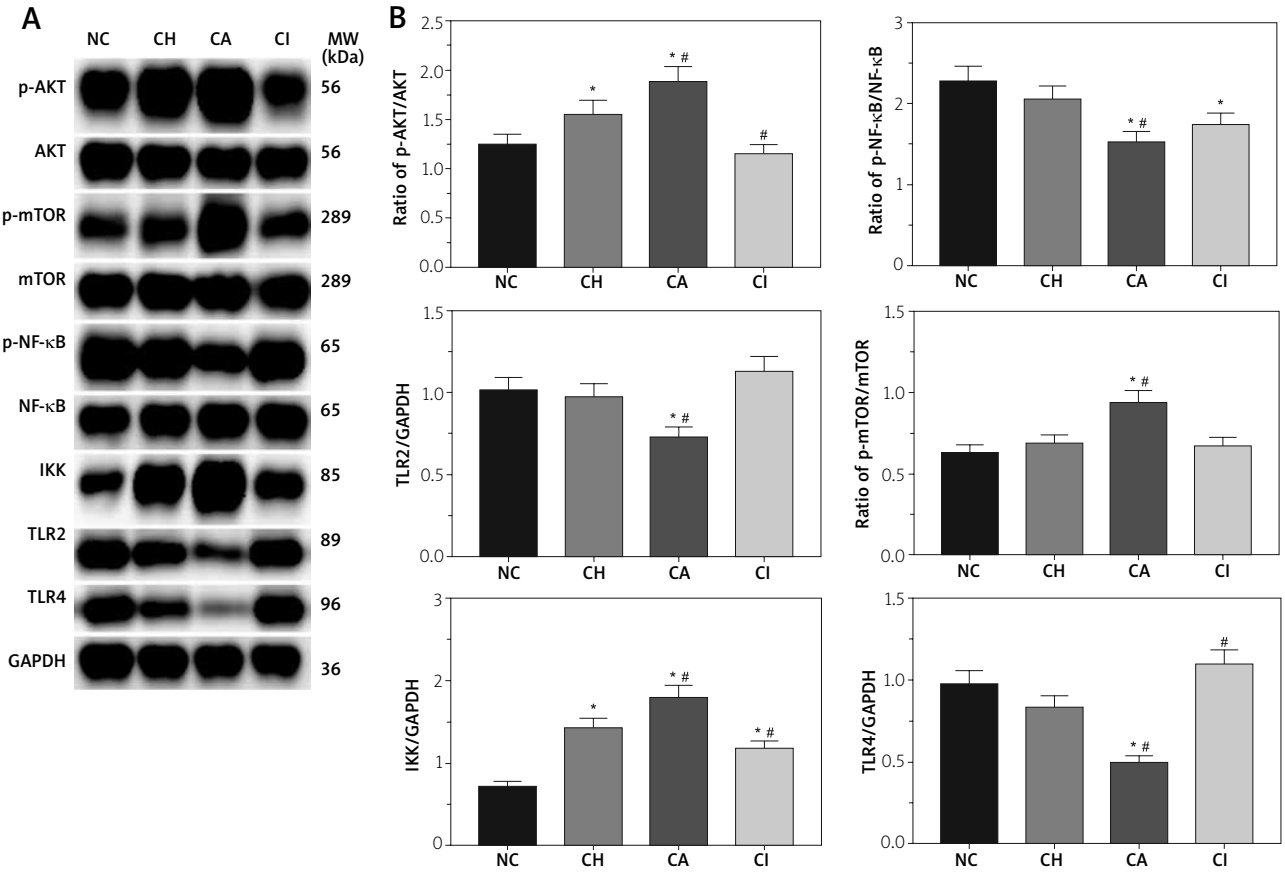

Fig. 9. Detection of activation of the PI3K/AKT/mTOR signalling pathway in GT1-7 cells using western blot analysis. **A**) Expression of key molecules in the PI3K/AKT/mTOR signalling pathway. **B**) Quantitative analysis of each protein. Data were presented as the mean ± SD. Each experiment was repeated three times independently (n = 3). *p < 0.05 compared with the NC group, #p < 0.05 compared with the CH group.

(p < 0.05) but was not significantly changed between the CH and CA groups. The expression of IKK in these groups was 0.95 ±0.08, 1.20 ±0.10, 1.56 ±0.13 and 0.64 ±0.05. Changes in the expression of IKK presented a similar trend with changes in the PI3K/AKT ratio. The expression of TLR2 in these groups was 1.04 ±0.09, 0.94 ±0.08, 0.68 ±0.06 and 2.04 ±0.17. Changes in the expression of TLR2 were significantly decreased in the CA group and significantly increased in the CI group compared with the NC and CH groups (p < 0.05). The expression of TLR4 in these groups was 2.51 ±0.21, 2.31 ±0.19, 1.88 ±0.16 and 2.20 ±0.18. Changes in the expression of TLR4 were significantly decreased in the CA group compared with the NC and CH groups (p < 0.05). As shown in Figure 9, the ratios of p-AKT/AKT in the NC, CH, CA and CI groups of GT1-7 cells were 1.25 ±0.10, 1.67 ±0.13, 1.83 ±0.14 and 1.16 ±0.09, respectively. The PI3K/AKT ratio was significantly increased in the CH and CA treatment groups compared with the NC group (p < 0.05). Compared with the CH group, the ratio of PI3K/AKT was significantly increased in the CA group and significantly decreased in the CI group (p < 0.05). The ratios of p-mTOR/mTOR in these groups were 0.63 ±0.05, 0.69 ±0.05, 0.94 ±0.07 and 0.67 ±0.05. The ratio of p-mTOR/mTOR was significantly increased in the CA group compared with the NC and CH groups (p < 0.05). The ratios of p-NF-κB/NF-κB in these groups were 2.28 ±0.18, 2.06 ±0.16, 1.54 ±0.12 and 1.75 ±0.13. The ratio of p-NF-κB/NF-κB was significantly decreased in the CA and CI groups compared with the NC group (p < 0.05) and significantly decreased in the CA group compared with the CH group (p < 0.05). The expression of IKK in these groups was 0.72 ±0.06, 1.43 ±0.11, 1.81 ±0.14 and 1.18 ±0.09. Changes in the expression of IKK presented a similar trend with

changes in the PI3K/AKT ratio. The expression of TLR2 in these groups was 1.02 ±0.08, 0.98 ±0.08, 0.74 ±0.06 and 1.13 ±0.09. Changes in the expression of TLR2 were significantly decreased in the CA group compared with the NC and CH groups ($p < 0.05$). The expression of TLR4 in these groups was 0.98 ±0.08, 0.84 ±0.06, 0.50 ±0.04 and 1.10 ±0.08. Changes in the expression of TLR4 were significantly decreased in the CA group compared with the NC and CH groups ($p < 0.05$) and significantly increased in the CI group compared with the CH group ($p < 0.05$).

Discussion

Atherosclerosis is a chronic low-grade sterile inflammatory process that occurs in arterial wells. The first step of atherosclerosis is disturbed laminar flow at arterial sites, followed by lipoprotein accumulation in endothelial cells [28]. The main cause of cerebral vessel disease is changes in blood components [10]. The occurrence of cerebral vessel disease is mainly related to hypertension and diabetes, especially hyperlipemia, which reflects dysfunction in cholesterol metabolism [11]. It is well known that for the prevention of risk factors for stroke, the control of cholesterol metabolism plays a critical role [5,53]. PI3K/AKT is a critical signalling pathway that regulates cellular proliferation, survival and death [12]. AKT also regulates the expression of mammalian target of rapamycin (mTOR) complex 1 (mTORC1), a key regulator of nutrient signalling, and controls cellular metabolism, translation and cellular responses [38]. A recent study indicated that AKT also regulates the expression of mTORC2, which also regulates the activation of AKT phosphorylation at the S473 site [46].

Recent studies noticed that the activation of a negative regulator of the mTOR signalling pathway, SIRT, leads to the inhibition of PARP1, further triggering the phosphorylation and activation of AKT [14]. In addition, pharmacological inhibition of PARP1 activates the PI3K/AKT signalling pathway, presenting a cytoprotective pathway by preventing the collapse of the mitochondrial membrane system under oxidative stress stimulation [45]. Another study found that inhibition of PARP1 further induced the phosphorylation of AKT in multiple target organs [47]. Macrophages are divided into two functional subtypes: the inflammatory or classically activated M1 subtype and the alternatively activated M2 subtype [15,25]. These two subtypes of macrophages can be reversibly shifted in different environments and different stages of atherosclerosis [42]. M1 macrophages secrete IL-12, IL-23 and tumor necrosis factor α (TNF-α), which are critical for protection from alien organisms, and M2 macrophages secrete IL-10, arginase I and chemokines, which are critical for inflammation, wound healing and tissue remodelling [25]. A previous study found that PI3K negatively regulates the process of macrophage activation and suppresses the anti-inflammatory response [7]. NF-κB is a downstream molecule of the PI3K/AKT signalling pathway, which is regulated by IKK. IKK interaction with mTORC2 further regulates the activity of the PI3K/AKT signalling pathway and promotes phosphorylation of AKT at the S473 site [6]. A previous study also found that knockout of IKK in mouse macrophages suppressed mTORC2 signalling and reduced AKT phosphorylation at the S473 site, indicating that AKT activation induces M2 macrophage activation, while AKT inhibition induces M1 macrophage activation [1]. However, the ratio of p-NF-κB/NF-κB was not significantly affected by inhibition of PARP1 in cells, indicating that inhibition of PARP1 performed a protective role against cholesterol stimulation *via* the PI3K/AKT/mTOR signalling pathway but was not dependent on NF-κB.

Toll-like receptors are part of the IL-1 receptor/Toll-like receptor subfamily, which contains an extracellular N-terminal-recognition domain. Among those subtypes, TLR2 and TLR4 are expressed by macrophages and neutrophils and have been considered to play an important role in the development of coronary artery disease (CAD) through the activation of the NF-κB pathway [4]. A previous study found that the expression of TLR2 is significantly increased in endothelial cells along with the expression of TLR1 and TLR4 [9]. In addition, an *in vitro* experiment found that the expression of TLR2 in endothelial cells exposed to laminar blood flow is lower than that under exposure to turbulent flow [8]. Researchers also proved that TLR2 deficiency leads to a reduction in atherosclerotic plaques in atherosclerosis-susceptible LDLR-deficient mice [30]. A human trial found that TLR4 expression in $CD14^+$ monocytes is increased in unstable angina and acute MI patients compared to control and stable angina patients [27], and activation of TLR4 is also related to heart failure [39]. The expression of TLR4 is elevated by oxLDL stimulation and is necessary for the differentiation of oxLDL-induced macrophages

into foam cells [17]. Decreased expression of TLR2 and TLR4 was observed after inhibition of PARP1, which has an anti-inflammatory function in cells. It is interesting that downregulation of PARP1 promotes the production of IL-10 *via* phosphorylation of the ERK signalling pathway, and both activation of the ERK signalling pathway and secretion of IL-10 were enhanced after the expression of PARP1 was interfered with [43]; thus, inhibition of PARP1 might present an anti-inflammatory effect by promoting the expression of IL-10.

ATP Binding Cassette Subfamily A Member 1 (ABCA1) and ATP Binding Cassette Subfamily G Member 1 (ABCG1) are two members of ATP binding cassette proteins and are under regulation of LXR alpha receptor at the transcription level [37], and perform a critical role in reverse cholesterol transport (RCT) by forming HDL particles and further affect metabolism of total cholesterol and HDL, even the development of atherosclerosis. ABCA1 and ABCG1 regulate the interaction of free CH with apolipoprotein A1 (ApoA1) and mature HDL particles [40], RCT from peripheral tissues to liver and excretion cholesterol with bile acids, which is mainly regulated by ABCA1 and ABCG1 as well as LDH biogenesis [18]. Previous studies found that knockdown of the expression of ABCA1 or ABCG1 leads to a reduction in lipid influx to the HDL fraction as well as HDL levels [31], induces the inflammatory response [49], and accelerates the development of atherosclerosis.

Recent studies found new capillaries in atherosclerotic plaques [13], indicating that angiogenesis is a critical step in the formation of atherosclerotic plaques and atherosclerotic complications [29]. A previous study found that the density of the vasa vasorum in atherosclerotic areas was higher than that in other areas, which indicates the early event of atherogenesis [43], and the application of angiogenesis factor inhibitors such as VEGF reduced the pace of plaque formation [16,36]. Thin-cap atheroma, macrophage infiltration and large necrotic cores are the main causes of intraplaque angiogenesis with haemorrhages. New capillaries in plaques are often leaky combined with the release of intraplaque erythrocytes and further induce atherosclerotic lesions in rabbits as well as the formation of foam cells [20].

FGF2 is a widely expressed 18 kDa protein that is released by injured cells or pathways independent of the endoplasmic reticulum-Golgi route. FGF2 is expressed by endothelial cells (ECs), vascular smooth muscle cells (VSMCs) and macrophages [21]. Exogenous application of FGF2 could improve endothelium-dependent relaxation by reducing the expression of vascular cell adhesion molecule-1 and decreasing the activation of endothelial cells and macrophages in atherosclerotic plaques. However, a previous study also found that after 10 weeks of a 2% hypercholesterolemic diet, FGF2 could no longer affect the function of endothelial cells [41]. Slow release of FGF2 in ApoE$^{-/-}$ mice could increase the density of vasa vasorum from 4 weeks as well as the progression of plaque formation [44].

A previous study found that the occurrence of autophagy is closely related to atherosclerosis in human and cell models. Using transmission electron microscopy (TEM), researchers found that autophagy occurs in major cell types of human atherosclerotic plaques [23]. In macrophages, autophagy could be stimulated by oxidized LDL and 7-ketocholeaterol *via* induction of ER stress in a direct or indirect method and promote the survival of macrophages by facilitating the clearance of protein and organelle damage and promoting the efflux of cholesterol from foam cells [33]. Mitophagy in macrophages can be activated by inflammasome activators, which require the relocation of p62 to mitochondria, limiting the inflammatory response regulated by NF-κB [52]. Deletion of Atg5 in macrophages results in the increased expression of ROS generation, leading to cellular apoptosis [22]. Deficiency in autophagy also impairs the cholesterol efflux function in macrophages with the increased secretion of IL-1β and cholesterol crystals and activates the NLR family pyrin domain containing 3 (NLRP3) inflammasome [35]. These results showed that inhibition of PARP1 might contribute to the anti-inflammatory effect, promoting the reverse transport of cholesterol and secretion of angiogenesis factors, indicating that inhibition of PARP1 expression might be a new therapeutic method in atherosclerosis.

Conclusions

Inhibition of PARP1 might be a therapeutic target in the treatment of cerebral vessels by promoting the anti-inflammatory effect, reversing the transport of cholesterol and secreting angiogenesis factors.

Limitation

The present study discovered the inhibition of PARP1 performed a protective role in atherosclero-

sis *via* inhibition of the accumulation of cholesterol and inflammation process in macrophages, however, the present study is the beginning of our research and only used the *in vitro* experiment, more experiments in animal models as well as clinical samples with large samples are needed in the further experiments to explore the application of PARP1 inhibition in treatment of cerebral vessels diseases. Besides, more experiments on the mechanism would also be performed using sequencing method to detect the detailed mechanism on PARP1 inhibition promoting the therapeutic effect on cerebral vessels diseases.

Funding

This project is supported by Qihang Fund Project of Fujian Medical University (2019QH1262); Natural Science Foundation of Fujian Province (2020J011273); Key R & D Projects of Zibo(2020ZC010247; 2020ZC010091)

Disclosure

The authors report no conflict of interest.

References

1. Babaev VR, Ding L, Zhang Y, May JM, Lin PC, Fazio S, Linton MF. Macrophage ikkαdeficiency suppresses akt phosphorylation, reduces cell survival, and decreases early atherosclerosis. Arterioscler Thromb Vasc Biol 2016; 36: 598-607.
2. Badimon L, Vilahur G, Padro T. Lipoproteins, platelets and atherothrombosis. Rev Esp Cardiol 2009; 62: 1161e1178.
3. Berger NA. Poly(ADP-ribose) in the cellular response to DNA damage. Radiat Res 1985; 101: 4-15.
4. Cole JE, Georgiou E, Monaco C. The expression and functions of toll-like receptors in atherosclerosis. Mediators Inflamm 2010; 2010: 393946.
5. Czuba E, Steliga A, Lietzau G, Kowiański P. Cholesterol as a modifying agent of the neurovascular unit structure and function under physiological and pathological conditions. Metab Brain Dis 2017; 32: 935-948
6. Dan HC, Antonia RJ, Baldwin AS. Pi3k/akt promotes feedforward mtorc2 activation through ikkα Oncotarget 2016; 7: 21064-21075.
7. Díaz-Guerra MJM, Castrillo A, Martín-Sanz P, Boscá L. Negative regulation by phosphatidylinositol 3-kinase of inducible nitric oxide synthase expression in macrophages. J Immunol 1999; 162: 6184-6190.
8. Dunzendorfer S, Lee HK, Tobias PS. Flow-dependent regulation of endothelial Toll-like receptor 2 expression through inhibition of SP1 activity. Circ Res 2004; 95: 684-691.
9. Edfeldt K, Swedenborg J, Hansson GK, Yan ZQ. Expression of toll-like receptors in human atherosclerotic lesions: a possible pathway for plaque activation. Circulation 2002; 105: 1158-1161.
10. Ezekowitz MD, Bridgers SL, James KE, Carliner NH, Colling CL, Gornick CC, Krause-Steinrauf H, Kurtzke JF, Nazarian SM, Radford MJ. Warfarin in the prevention of stroke associated with nonrheumatic atrial fibrillation. Veterans Affairs Stroke Prevention in Nonrheumatic Atrial Fibrillation Investigators. N Engl J Med 1992; 327: 1406-1412.
11. Fisher CM. Lacunes: small, deep cerebral infercts. Neurology 1965; 15: 774-778.
12. 25. Fisher EA. Regression of atherosclerosis. Arterioscler Thromb Vasc Biol 2016; 36: 226-235.
13. Fruman DA, Chiu H, Hopkins BD, Bagrodia S, Cantley LC, Abraham RT. The pi3k pathway in human disease. Cell 2017; 170: 605-635.
14. Geiringer E. Intimal vascularization and atherosclerosis. J Pathol Bacteriol 1951; 63: 201-211.
15. Giulia P, Arcangela GM, Bruno M, Elvira DM, Luciano M, Laura M. PARP1 inhibition affects pleural mesothelioma cell viability and uncouples AKT/mTOR axis via SIRT1. J Cell Mol Med 2013; 17: 233-241.
16. Gordon S, Martinez FO. Alternative activation of macrophages: Mechanism and functions. Immunity 2010; 32: 593–604.
17. Gossl M, Herrmann J, Tang H, Versari D, Galili O, Mannheim D, Rajkumar SV, Lerman LO, Lerman A. Prevention of vasa vasorum neovascularization attenuates early neointima formation in experimental hypercholesterolemia. Basic Res Cardiol 2009; 104: 695-706.
18. Howell KW, Meng X, Fullerton DA, Jin CH, Reece TB, Cleveland JC. Toll-like receptor 4 mediates oxidized LDL-induced macrophage differentiation to foam cells. J Surg Res 2011; 171: e27-31.
19. Jessup W, Gelissen IC, Gaus K, Kritharides L. Roles of ATP binding cassette transporters A1 and G1, scavenger receptor BI and membrane lipid domains in cholesterol export from macrophages. Curr Opin Lipidology 2006; 17: 247-257.
20. Jong SK. Role of blood lipid levels and lipid-lowering therapy in stroke patients with different levels of cerebral artery diseases: reconsidering recent stroke guidelines. J Stroke 2021; 23: 149-161.
21. Kolodgie FD, Gold HK, Burke AP, Fowler DR, Kruth HS, Weber DK, Farb A, Guerrero LJ, Hayase M, Kutys R, Narula J, Finn AV, Virmani R. Intraplaque hemorrhage and progression of coronary atheroma. N Engl J Med 2003; 349: 2316-2325.
22. Li D, Zhang C, Song F, Lubenec I, Tian Y, Song QH. VEGF regulates FGF-2 and TGF-beta1 expression in injury endothelial cells and mediates smooth muscle cells proliferation and migration. Microvasc Res 2009; 77: 134e42.
23. Liao X, Sluimer JC, Wang Y, Subramanian M, Brown K, Pattison JS, Robbins J, Martinez J, Tabas I. Macrophage autophagy plays a protective role in advanced atherosclerosis. Cell Metabolism 2012; 15: 545-553.
24. Liu H, Cao Y, Tong T, Shi JJ, Zhang YL, Yang YP, Liu CF. Autophagy in atherosclerosis: a phenomenon found in human carotid atherosclerotic plaques. Chin Med J 2015; 128: 69-74.
25. Livak KJ, Schmittgen TD. Analysis of relative gene expression data using real-time quantitative PCR and the 2(-Delta Delta C(T)) method. Methods 2001; 25: 402-408.
26. Manning BD, Cantley LC. Akt/pkb signaling: Navigating downstream. Cell 2007; 129: 1261-1274.

27. Mehta D, Malik AB. Signaling mechanisms regulating endothelial permeability. Physiol Rev 2006; 86: 279e367.
28. Methe H, Kim JO, Kofler S, Weis M, Nabauer M, Koglin J. Expansion of circulating Toll-like receptor 4-positive monocytes in patients with acute coronary syndrome. Circulation 2005; 111: 2654-2661.
29. Moore KJ, Tabas I. Macrophages in the pathogenesis of atherosclerosis. Cell 2011; 145: 341-355.f
30. Moreno PR, Purushothaman KR, Sirol M, Levy AP, Fuster V. Neovascularization in human atherosclerosis. Circulation 2006; 113: 2245-2252.
31. Mullick AE, Tobias PS, Curtiss LK. Modulation of atherosclerosis in mice by Toll-like receptor 2. J Clin Invest 2005; 115: 3149-3156.
32. Orso E, Broccardo C, Kaminski WE, Böttcher A, Liebisch G, Drobnik W, Götz A, Chambenoit O, Diederich W, Langmann T, Spruss T, Luciani MF, Rothe G, Lackner KJ, Chimini G, Schmitz G. Transport of lipids from golgi to plasma membrane is defective in tangier disease patients and Abc1-deficient mice. Nat Genet 2000; 24: 192-196.
33. Oumouna-Benachour K, Hans CP, Suzuki Y, Naura A, Datta R, Belmadani S, Fallon K, Woods C, Boulares AH. Poly(ADP-ribose) polymerase inhibition reduces atherosclerotic plaque size and promotes factors of plaque stability in apolipoprotein E-deficient mice: Effects on macrophage recruitment, nuclear factor-kappaB nuclear translocation, and foam cell death. Circulation 2007; 115: 2442-2450.
34. Ouimet M, Franklin V, Mak E, Liao X, Tabas I, Marcel YL. Autophagy regulates cholesterol efflux from macrophage foam cells via lysosomal acid lipase. Cell Metabolism 2011; 13: 655-667.
35. Radovits T, Lin LN, Zotkina J, Gero D, Szabó C, Karck M, Szabó G. Poly(ADP-ribose) polymerase inhibition improves endothelial dysfunction induced by reactive oxidant hydrogen peroxide in vitro. Eur J Pharmacol 2007; 564: 158-166.
36. Razani B, Feng C, Coleman T, Emanuel R, Wen HT, Hwang S, Ting JP, Virgin HW, Kastan MB, Semenkovich CF. Autophagy links inflammasomes to atherosclerotic progression. Cell Metabolism 2012; 15: 534–544.
37. Ritman EL, Lerman A. The dynamic vasa vasorum. Cardiovasc Res 2007; 75: 649-658.
38. Rosenson RS, Brewer HB, Davidson WS, Fayad ZA, Fuster V, Goldstein J, Hellerstein M, Xian-Cheng Jiang, Michael C Phillips, Daniel J Rader, Alan T Remaley, George H Rothblat, Tall AR, Yvan-Charvet L. Cholesterol efflux and atheroprotection: advancing the concept of reverse cholesterol transport. Circulation 2012; 125: 1905-1919.
39. Sabatini DM. Twenty-five years of mTOR: Uncovering the link from nutrients to growth. Proc Natl Acad Sci U S A 2017; 114: 11818-11825.
40. Satoh M, Shimoda Y, Maesawa C, Akatsu T, Ishikawa Y, Minami Y, Hiramori K, Nakamura M. Activated toll-like receptor 4 in monocytes is associated with heart failure after acute myocardial infarction. Int J Cardiol 2006; 109: 226-234.
41. Singaraja RR, Fievet C, Castro G, James ER, Hennuyer N, Clee SM, Bissada N, Choy JC, Fruchart JC, McManus BM, Staels B, Hayden MR. Increased ABCA1 activity protects against atherosclerosis. J Clin Invest 2002; 110: 35-42.
42. Six I, Mouquet F, Corseaux D, Bordet R, Letourneau T, Vallet B, Dosquet CC, Dupuis B, Jude B, Bertrand ME, Bauters C, Van Belle E. Protective effects of basic fibroblast growth factor in early atherosclerosis. Growth Factor 2004; 22: 157e67.
43. Stout RD, Jiang C, Matta B, Tietzel I, Watkins SK, Suttles J. Macrophages sequentially change their functional phenotype in response to changes in microenvironmental influences. J Immunol 2005; 175: 342-349.
44. Su XP, Ye LL, Chen XX, Zhang HD, Zhou Y, Ding XK, Chen D, Lin QA, Chen CS. MiR-199-3p promotes ERK-mediated IL-10 production by targeting poly (ADP-ribose) Polymerase-1 in patients with systemic lupus erythematosus. Chem Biol Interact 2019; 306: 110-116.
45. Tanaka K, Nagata D, Hirata Y, Tabata Y, Nagai R, Sata M. Augmented angiogenesis in adventitia promotes growth of atherosclerotic plaque in apolipoprotein E-deficient mice. Atherosclerosis 2011; 215: 366e73.
46. Tapodi A, Debreceni B, Hanto K, Bognar Z, Wittmann I, Gallyas F, Varbiro G, Sumegi B. Pivotal role of Akt activation in mitochondrial protection and cell survival by poly(ADPribose)polymerase-1 inhibition in oxidative stress. J Biol Chem 2005; 280: 35767-35775.
47. Thobe K, Sers C, Siebert H. Unraveling the regulation of mtorc2 using logical modeling. Cell Commun Signal 2017; 15: 6.
48. Veres B, Gallyas F, Varbiro G, Berente Z, Osz E, Szekeres G, Szabo C, Sumegi B. Decrease of the inflammatory response and induction of the Akt/protein kinase B pathway by poly-(ADP-ribose) polymerase 1 inhibitor in endotoxin-induced septic shock. Biochem Pharmacol 2003; 65: 1373-1382.
49. Wei SJ, Xing JH, Wang BL, Xue L, Wang JL, Li R, Qin WD, Wang J, Wang XP, Zhang MX, Chen YG. Poly(ADP-ribose) polymerase inhibition prevents reactive oxygen species induced inhibition of aldehyde dehydrogenase 2 activity. Biochim Biophys Acta 2013; 1833: 479-486.
50. Yvan-Charvet L, Wang N, Tall AR. The role of HDL, ABCA1 and ABCG1 transporters in cholesterol efflux and immune responses. Arterioscler Thromb Vasc Biol 2010; 30: 139-143.
51. Zha SY, Wang F, Li Z, Ma ZY, Yang L, Liu F. PJ34, a PARP1 inhibitor, promotes endothelial repair in a rabbit model of high fat diet-induced atherosclerosis. Cell Cycle 2019; 18: 2099-2109.
52. Zheng P, Ding YZ, Lu FY, Liu NN, Wu HF, Bian ZP, Chen XJ, Yang D. Atorvastatin reverses high cholesterol-induced cardiac remodelling and regulates mitochondrial quality-control in a cholesterol-independent manner: An experimental study. Clin Exp Pharmacol Physiol 2021; 48: 1150-1161.
53. Zhong Z, Umemura A, Sanchez-Lopez E, Liang S, Shalapour S, Wong J, He F, Boassa D, Perkins G, Ali SR, McGeough MD, Ellisman MH, Seki E, Gustafsson AB, Hoffman HM, Diaz-Meco MT, Moscat J, Karin M. NF-κB restricts inflammasome activation via elimination of damaged mitochondria. Cell 2016; 164: 896-910.
54. Zimmer S, Grebe A, Latz E. Danger signaling in atherosclerosis. Circ Res 2015; 116: 323-340.